Published in final edited form as:
Circulation. 2005 January 4; 111(1): 21–29. doi:10.1161/01.CIR.0000151291.32974.D5.

Transgenic Mouse Model of Ventricular Preexcitation and Atrioventricular Reentrant Tachycardia Induced by an AMP-Activated Protein Kinase Loss-of-Function Mutation Responsible for Wolff-Parkinson-White Syndrome

Jasvinder S. Sidhu, MD, **Yadavendra S. Rajawat, MD**, **Tapan G. Rami, MD**, **Michael H. Gollob, MD**, **Zhinong Wang, MD, PhD**, **Ruiyong Yuan, MD**, **A.J. Marian, MD**, **Francesco J. DeMayo, MD**, **Donald Weilbacher, MD**, **George E. Taffet, MD**, **Joanna K. Davies, PhD**, **David Carling, PhD**, **Dirar S. Khoury, PhD**, and **Robert Roberts, MD**
Baylor College of Medicine (J.S.S., Y.S.R., T.G.R., Z.Q., R.Y., A.J.M., F.J.D., D.W., G.E.T., D.S.K.), Houston, Tex; University of Ottawa Heart Institute (M.H.G., R.R.), Ottawa, Ontario, Canada; and Imperial College (J.K.D., D.C.), London, England

Abstract

Background—We identified a gene (*PRKAG2*) that encodes the γ-2 regulatory subunit of AMP-activated protein kinase (AMPK) with a mutation (Arg302Gln) responsible for familial Wolff-Parkinson-White (WPW) syndrome. The human phenotype consists of ventricular preexcitation, conduction abnormalities, and cardiac hypertrophy.

Methods and Results—To elucidate the molecular basis for the phenotype, transgenic mice were generated by cardiac-restricted expression of the wild-type (TG_{WT}) and mutant(TG_{R302Q}) *PRKAG2* gene with the cardiac-specific promoter α-myosin heavy chain. ECG recordings and intracardiac electrophysiology studies demonstrated the TG_{R302Q} mice to have ventricular preexcitation (PR interval 10±2 versus 33±5 ms in TG_{WT}, $P<0.05$) and a prolonged QRS (20±5 versus 10±1 ms in TG_{WT}, $P<0.05$). A distinct AV accessory pathway was confirmed by electrical and pharmacological stimulation and substantiated by induction of orthodromic AV reentrant tachycardia. Enzymatic activity of AMPK in the mutant heart was significantly reduced (0.009±0.003 versus 0.025±0.001 nmol $\cdot$ min^{-1} $\cdot$ g^{-1} in nontransgenic mice), presumably owing to the mutation disrupting the AMP binding site. Excessive cardiac glycogen was observed. Hypertrophy was confirmed by increases in heart weight (296 versus 140 mg in TG_{WT}) and ventricular wall thickness.

Conclusions—We have developed a genetic animal model of WPW that expresses a mutation responsible for a familial form of WPW syndrome with a phenotype identical to that of the human, including induction of supraventricular arrhythmia. The defect is due to loss of function of AMPK. Elucidation of the molecular basis should provide insight into development of the cardiac conduction system and accessory pathways.

Keywords

Wolff-Parkinson-White syndrome; genetics; tachycardia

Correspondence to Robert Roberts, MD, University of Ottawa Heart Institute, 40 Ruskin St, Ottawa, Ontario, Canada K1Y 4W7. rroberts@ottawaheart.ca.

Wolff-Parkinson White syndrome (WPW) has remained a fascination for the cardiologist, particularly for the electrophysiologist. This is in part because WPW is the sina quo non of reentry as a mechanism responsible for arrhythmias. Reentry predominates as the mechanism for arrhythmias in the atria and ventricles from many different causes. Although the molecular basis for this disorder has remained unknown, extensive anatomic, electrical, and physiological research has been pursued in humans.[1] Research in humans has targeted the accessory pathway that bypasses the atrioventricular (AV) node and is responsible for the short PR interval with a slurring of the initial segment of the QRS complex, known as a delta wave. This syndrome is the second most common cause of supraventricular arrhythmias in the Western world and the most common cause in Asian countries such as China.[2] Although it is usually associated with symptoms such as palpitations and presyncope, if sustained, it can induce symptoms of heart failure. It is also known to initiate atrial fibrillation, which may deteriorate into sudden death.[3] The accessory pathway bypassing the AV node is in itself a curiosity. Several such accessory pathways are present at birth, but they coalesce or are absorbed (apoptosis) over the subsequent weeks or months.[4] Thus, the presence of the accessory pathway in adulthood presumably reflects some cardiac developmental abnormality.

We were surprised to find that the genetic defect responsible for WPW in families we have studied[5] was a missense mutation in the gene *PRKAG2* that encodes for the γ-2 subunit of AMPK (AMP-activated protein kinase).[5] Subsequently, other investigators[6–8] have shown the gene to be responsible for WPW in many other families. The functions of AMPK are pleiotropic. Through its action of phosphorylation, it plays a major role in the synthesis and distribution of ATP primarily by regulating carbohydrate and fatty acid metabolism.[9] AMPK mediates many of the actions of leptin and adiponectin and of the oral diabetic drugs, such as metformin.[9] To explore the molecular basis whereby this defect generates a phenotype of WPW and reentrant arrhythmias, we generated a transgenic mouse model by expressing the human mutant *PRKAG2* gene. The mouse exhibited a phenotype of preexcitation, inducible orthodromic AV reentrant tachycardia, cardiac hypertrophy, and excessive cardiac glycogen, as observed in the human phenotype. Using this model, we have shown the primary molecular defect is loss of cardiac AMPK activity. This appears to be due to the mutation disrupting the γ-2 subunit binding site for AMP, which is required for activation of AMPK activity. The model provides a means to further elucidate the molecular network that leads to development of the accessory pathway (preexcitation), supraventricular arrhythmias, and hypertrophy.

Methods

Transgene Construct

The transgene construct consisted of an α-myosin heavy chain (MHC) promoter, PRKAG2 cDNA, 3′UTR human growth hormone. The construct was generated by placing an insert (PRKAG2 cDNA) within the cloning site of a cassette that contained the α-MHC promoter and a 3′UTR human growth hormone. To obtain a PRKAG2 cDNA, human RNA was converted to cDNA and amplified by reverse transcription polymerase chain reaction (RTPCR). A *Sal*I restriction site was attached at each end of the cDNA fragment. Site-directed mutagenesis was used to generate a missense mutation that resulted in a substitution of an arginine for glutamine at amino acid residue 302, a mutation responsible for familial WPW in humans.[10] The cDNA was subcloned and sequenced from end to end. Inserts containing mutated PRKAG2 cDNA and wild-type PRKAG2 cDNA were excised with *Sal*I restriction enzymes and reinserted into the α-MHC cassette. PCR and direct sequencing were performed to determine whether the insert was in the correct direction. The transgene construct that contained the α-MHC promoter, PRKAG2 cDNA, and 3′UTR human growth hormone was then released by *Bam*HI.

Generation of Transgenic Mice

Multiple injections of PRKAG2 cDNA were performed to develop 3 lines of transgenics that expressed the mutant gene, substitution of arginine for glutamine at residue 302 (referred to as TG_{R302Q} mice), and 2 lines of transgenics that expressed the normal human cDNA, referred to as the wild type (TG_{WT}). Linearized transgene was microinjected into fertilized FVB mouse oocytes.

Genotyping

Founders of each transgenic line were identified by PCR screening. The primers, specific for the human PRKAG2 cDNA, in the forward direction were 5′-GGGCATCAGGTTTTTCTCTCCCGCTCCA-3′ and in the reverse direction, 5′-CCATAGGTGATTTATAGTATCTATGTAG-3′. PCR was performed on the genomic DNA isolated from biopsies of the mice tails with the QIAGEN DNeasy kit, and the product was sequenced.

Transgene Expression

Expression of the transgene in the heart was assessed by RTPCR and Northern blot analysis. Mouse myocardial tissue was homogenized in Trizol reagent and the RNA ethanol precipitated from the homogenate. One-step RTPCR was performed on RNA from TG_{WT} and TG_{R302Q} mice. Primers mentioned previously were used to amplify DNA, and the products were sequenced. Northern blot analysis was preformed with a probe specific for the human γ-2 subunit cDNA. Ten micrograms of RNA was loaded on denaturing RNA gel and transferred to a blotting membrane. Membranes were then probed with ^{32}P-labeled human specific probes by the rapid hybridizing technique. The membrane with labeled probe was overlaid with radiographic film and exposed overnight at −70°C.

Myocardial AMPK Enzymatic Activity

Homogenates of heart from TG_{WT} and TG_{R302Q} mice were obtained to isolate AMPK. The AMPK protein was immunoprecipitated from the homogenate with either an antibody specific for the γ-2 subunit or an antibody that recognizes both the β-1 and β-2 subunits (pan-β). In each case, the antibodies (γ-2 or pan β-2) cross-react with both human and mouse AMPK. Enzymatic activity was determined in the absence or presence of 0.2 mmol/L AMP as described previously[11] and reported in nmol $\cdot$ min^{-1} $\cdot$ g^{-1} wet weight.

Histopathology

Mouse hearts were removed, weighed, and fixed in 10% formalin. Total body weight was recorded, and heart weight was expressed as a ratio. One-micrometer sections of the hearts were prepared and stained with hematoxylin and eosin stain or periodic acid Schiff (PAS). PAS staining was used to determine whether there was deposition of glycogen.

Markers of Hypertrophy

Molecular markers (atrial natriuretic peptide and brain natriuretic peptide) known to be expressed during cardiac hypertrophy were assessed by Northern blot analysis. Analysis was performed on myocardial samples from $TG_{R302Q,}$ TG_{WT}, and nontransgenic mice.

Echocardiography

Mice were anesthetized by isoflurane inhalation (isoflurane 1.5%, oxygen 98.5%). Limbs were attached to electrodes for ECG monitoring. M-mode echocardiographs of the left ventricle were recorded at the tip of the mitral valve apparatus with a 5- to 7.5-MHz transducer. Septal and posterior wall thickness, left ventricular end-systolic diameter (ESD),

and left ventricular end-diastolic diameter (EDD) were measured, and percent fractional shortening was calculated as (EDD−ESD)/EDD as described previously.[12]

Electrocardiography and Electrophysiology Studies

For ECG screening, mice were anesthetized by intraperitoneal injection (15 mL/kg) of a mixture of sodium pentobarbital (6.61 mg/mL), sodium chloride (4.13 mg/mL), and ethanol (0.18 mL/mL). A body-surface ECG (leads I, II, and III) was recorded in 134 TG_{R302Q} mice starting at 35±16 days of age and in 41 TG_{WT} mice at 88±3 days of age. The ECG was filtered between 0.5 and 500 Hz and sampled at 1 kHz (model MP100, BIOPAC Systems).

To conduct electrophysiology studies, mice were anesthetized, and 6 limb leads were continuously recorded. An 8-electrode lumen catheter (1.1F, model EPR-801, Millar Instruments, or 2F, model CIBer, NuMED) was inserted through the jugular vein and advanced into the right atrium and ventricle for pacing and recording. The ECG was filtered between 5 and 100 Hz, and intracardiac electrograms were filtered between 5 and 500 Hz, whereas the sampling rate was set at 1 kHz on all signals (CardioLab, GE Medical Systems). Electrophysiology methods similar to standard clinical electrophysiology studies were performed as described previously.[13] Electrical stimulation was applied through the catheter electrodes with an external stimulator (model S8800; AstroMed). After a period of baseline rhythm, decremental atrial pacing was applied whereby the cycle length was repeatedly shortened by 10 ms, starting from a pacing cycle length of 20 ms less than the intrinsic sinus cycle length, until continuous atrial capture could not be maintained. After 10 seconds of pacing at each cycle length, sinus node recovery time was determined as the longest pause from the last paced atrial depolarization to the first sinus return cycle. Atrial pacing cycle lengths resulting in Wenckebach and 2:1 AV conduction were also noted. Subsequently, refractory periods were determined by delivering an 8-stimulus drive train (S1) at a cycle length of 100 ms followed by a premature stimulus (S2) that was progressively decremented in 10-ms intervals. The effective refractory period was defined as the longest S1-S2 coupling interval that failed to generate a propagated beat with S2 in 2 separate attempts. Inducibility of arrhythmias was investigated by delivering 2 extrastimuli (S2 and S3) that were programmed at progressively shorter intervals after a drive train (S1). Procainamide was administered intravenously (30 mg/kg) to further confirm the presence of accessory pathways.

Statistical Analysis

Continuous variables were expressed as mean±SD. Differences between TG_{R302Q} and TG_{WT} mice were compared by Student's *t* test. ANOVA was applied for multiple comparisons.

Results

Genotype and Expression of *PRKAG2* in Transgenic Mice

One hundred forty mice were transgene positive in the 3 mutant lines, and 50 mice were transgene positive in the 2 wild-type lines. Expression of the transgene was confirmed at the RNA level by Northern analysis (Figure 1). The mouse heart was assessed for protein expression by determining AMPK enzymatic activity in TG_{WT}, TG_{R302Q}, and nontransgenic mice as indicated subsequently (Figure 2).

Histology of Transgenic Mice

TG_{WT} mice, TG_{R302Q} mice, and controlled nontransgenic mice were matched for gender and age to compare cardiac mass. The average body weight was similar (28, 24, and 26 g for mutant, wild-type, and nontransgenic mice, respectively). In contrast, the weight of the

mutant hearts averaged 296.67 mg, which was twice that of the wild-type mice (140 mg, $P<0.001$) and nearly 3 times that of the nontransgenic mice (117 mg, $P<0.001$). Gross appearance of the hearts appeared normal except for the increase in size of the TG_{WT} and TG_{R302Q}. Hematoxylin-and-eosin stains showed that myocytes of the TG_{R302Q} and TG_{WT} mice exhibited multiple nuclei with great variation in size, in keeping with hypertrophy. These changes were observed consistently throughout the right and left ventricles of the wild-type and mutant mice. In the mutant mice, large vacuoles were abundant throughout the myocardium of the right and left ventricles. PAS staining confirmed the vacuoles were filled with PAS-positive material indicating glycogen (Figures 3 and 4). Myocytes containing glycogen were abundant in the myocardium of the right and left ventricles of the mutant mice but were not present in wild-type or nontransgenic mice. Histology of the myocardium was normal in nontransgenic mice. In the mutant mice, muscle bundles that extended from the atrium to the ventricle in the region of the fibrous body were observed, but it remains to be determined whether these are the accessory pathways responsible for electrical conduction bypassing the AV node.

Myocardial AMPK Enzymatic Activity

Enzymatic activity of AMPK in the heart was assessed after immunoprecipitation of the protein. After immunoprecipitation with anti-γ-2 antibodies, myocardial AMPK activity averaged 0.002±0.001 nmol $\cdot$ $min^{-1} \cdot g^{-1}$ wet weight in TG_{R302Q} mice, 0.009±0.003 nmol $\cdot$ $min^{-1} \cdot g^{-1}$ wet weight in TG_{WT} mice, and 0.025±0.02 nmol $\cdot$ $min^{-1} \cdot g^{-1}$ wet weight in nontransgenic mice (Figure 2). AMP had no significant effect on AMPK activity under these conditions, similar to a previous study.[9] Thus, TG_{R302Q} mice enzymatic activity was only 22% of that of transgenic wild type and <4% of that of nontransgenic mice, which is in keeping with loss of function of AMPK. Despite the presence of AMP, enzymatic activity did not increase significantly. This is in keeping with the mutation disrupting the γ-2 subunit binding site for AMP. To determine total AMPK activity in the heart extracts, AMPK complexes were immunoprecipitated with an antibody that recognizes both β-1 and β-2 (Figure 2). With this assay, TG_{R302Q} mice enzymatic activity was 17% of that of TG_{WT} (0.005±0.003 versus 0.029±0.019 nmol $\cdot$ $min^{-1} \cdot g^{-1}$) and 5% of that of nontransgenic mice (0.094±0.058 nmol $\cdot$ $min^{-1} \cdot g^{-1}$). Relative levels of AMPK activity in the hearts were almost identical to those obtained with the γ-2 antibodies, and these results demonstrate that the γ-2 mutation results in a loss of function of AMPK.

Markers of Cardiac Hypertrophy

Densitometry shows a 2-fold increase of brain natriuretic peptide present in mutant mice over that in nontransgenic and transgenic wild-type mice. There was no increase in atrial natriuretic peptide observed in either the mutant or transgenic wild-type mice over that in the nontransgenic mice. There was no correlation with gender.

Echocardiographic Assessment

Echocardiography was performed in 15 wild-type, 12 mutant, and 11 nontransgenic mice (Table). The hearts of the TG_{R302Q} and TG_{WT} mice were hypertrophied, with posterior wall thickness averaging 0.13 cm for TG_{WT} mice (age 2 months) and 0.12 in the TG_{R302Q} transgenic mice (age 2 months) compared with 0.09 for nontransgenics ($P<0.001$). There was no significant difference between posterior wall thickness of TG_{WT} and TG_{R302Q} mice. There was an increased end-diastolic diameter and end-systolic diameter in both TG_{WT} and TG_{R302Q} mice with decreased systolic function.

Phenotype Characterization by Electrocardiography and Electrophysiology

An ECG (Figure 5) identified 21 TG_{R302Q} mice manifesting ventricular preexcitation at 51±29 days of age, as evidenced by a short PR interval (10±2 versus 33±5 ms in TG_{WT}; $P<0.001$) and wide QRS (20±5 versus 10±1 ms in TG_{WT}; $P<0.001$). Figure 6 summarizes the distribution of 134 TG_{R302Q} mice with and without ventricular preexcitation according to age. ECG recordings were repeated in 12 TG_{R302Q} mice with manifest ventricular preexcitation, and maintenance of preexcitation was confirmed in all mice during observation up to 225 days of age.

An electrophysiology study was performed on 12 TG_{R302Q} mice with manifest ventricular preexcitation and on 11 TG_{WT} mice. TG_{R302Q} mice showed significant prolongation in the sinus cycle length (176±41 versus 118±20 ms in TG_{WT}, $P<0.001$), whereas sinus node recovery times were similar (43±27 versus 45±16 ms in TG_{WT}, P=NS).

Evidence of an accessory pathway outside the AV node in TG_{R302Q} mice was confirmed by atrial programmed electrical stimulation. Decremental atrial pacing resulted in fixed AV conduction in TG_{R302Q} mice until accessory pathway refractoriness was reached, whereas TG_{WT} mice exhibited normal AV nodal response characterized by gradual prolongation in AV conduction. During atrial extrastimulation (Figure 7), blockade of the accessory pathway by a premature stimulus was accompanied by a prolonged PR interval (29±8 ms) and a narrow QRS duration (12±2 ms), which is consistent with normal conduction over the AV node. The accessory pathway refractory period was 76±9 ms, and the AV node refractory period in TG_{R302Q} mice was 44±9 ms (53±11 ms in TG_{WT}, P=NS). The longest atrial pacing cycle length in TG_{R302Q} mice that resulted in AV nodal Wenckebach periodicity was 70±5 ms (71±8 ms in TG_{WT}, P=NS) and the longest that resulted in AV nodal 2:1 conduction was 58±8 ms (61±9 ms in TG_{WT}, P=NS). The atrial effective refractory period in TG_{R302Q} mice was 43±8 ms (45±10 ms in TG_{WT}, P=NS).

Retrograde VA conduction over the accessory pathway was confirmed in TG_{R302Q} mice by decremental ventricular pacing, which resulted in fixed VA conduction. Ventricular programmed electrical stimulation showed that the ventricular refractory period was significantly prolonged in TG_{R302Q} mice (63±6 versus 44±15 ms in TG_{WT} mice, P=0.024).

Induction of Orthodromic AV Reentrant Tachycardia

Atrial electrical stimulation induced supraventricular tachycardia in 6 of 12 TG_{R302Q} mice and was consistent with orthodromic AV reentrant tachycardia characterized by antegrade conduction via the AV node and retrograde conduction over the accessory pathway (Figure 8). Only single reentrant beats could be induced in 4 other TG_{R302Q} mice. Reentrant beats or tachycardia could not be induced in 2 TG_{R302Q} mice. Induced tachycardia duration ranged from 2 to 64 beats, with an average cycle length of 69±2 ms. The VA interval during tachycardia (18±4 ms) was similar to that during ventricular pacing (19±5 ms). Reentrant tachycardia could not be induced by ventricular electrical stimulation. Reentrant single beats or tachycardia could not be induced in TG_{WT} mice.

Atrial premature beats and/or tachycardia were observed spontaneously or after atrial electrical stimulation in 7(58%) of 12 TG_{R302Q} mice and in 3 (27%) of 11 TG_{WT} mice. Ventricular electrical stimulation did not induce ventricular arrhythmias in either TG_{R302Q} or TG_{WT} mice.

Pharmacological Blockade

Procainamide blocked the accessory pathway in TG_{R302Q} mice within 3 to 5 minutes of administration. As illustrated in Figure 9, procainamide resulted in sudden prolongation of

the PR interval from 11±4 to 27±6 ms and narrowing of the QRS duration from 17±3 to 13±3 ms (n = 8). These sudden ECG changes were not observed in TG_{WT} mice after procainamide administration. Procainamide has been documented in many studies to block conduction in the accessory pathway with relative sparing of AV nodal conduction.[14,15]

Discussion

We generated a transgenic mouse that expressed the human *PRKAG2* gene containing the mutation R302Q, which is responsible for a phenotype of WPW, conduction system disease, and ventricular hypertrophy with excessive cardiac glycogen. The presence of a functioning accessory pathway bypassing the AV node giving rise to the WPW was demonstrated in TG_{R302Q} mice by the following diagnostic criteria: (1) baseline ECG recordings exhibited a short PR interval and increased QRS duration with slurred upstroke; (2) atrial pacing blocked the accessory pathway at a long refractory period and was accompanied by immediate prolongation of the PR interval and shortening of the QRS duration (consistent with conduction through the AV node); (3) atrial pacing at a critical cycle length reproducibly provoked AV reentrant beats and tachycardia with antegrade conduction through the AV node and retrograde conduction via the accessory pathway; (4) ventricular pacing resulted in a fixed short VA interval and was similar to the VA interval during reentrant beats or tachycardia (in line with retrograde conduction through the accessory pathway); and (5) procainamide blocked the accessory pathway and abolished ventricular preexcitation, as demonstrated by sudden lengthening of the PR interval and abbreviation of QRS duration (in agreement with normal conduction through the AV node). In keeping with extensive experience,[16,17] anesthesia did not affect identification of the accessory pathways. The mutant hearts showed abundant myocardial glycogen. Ventricular hypertrophy was confirmed by a significant increase in weight of the TG_{WT} hearts and more than a doubling of the heart weight in TG_{R302Q} mice. This was confirmed by echocardiographic analysis that showed increased thickness of the posterior wall. Thus, the phenotype of our animal model is virtually identical to the human phenotype.

AMPK, a metabolic sensor of ATP stores, makes ATP available in response to the cell's energy demands.[9] It inhibits glycogen synthase, which increases the availability of glucose for energy production. Glycogen deposition was markedly increased in the TG_{R302Q} hearts, similar to that observed in the human phenotype.[6] A similar increase in cardiac glycogen deposition was observed by Arad et al[10] in their transgenic model expressing the N488I missense mutation in the *PRKAG2* gene. The present in vivo studies showed minimal cardiac AMPK activity in the transgenic mutant mice, consistent with results of in vitro studies. In vitro studies by Daniel and Carling[18] showed marked attenuation or absent enzymatic activity associated with the R302Q mutation. Further in vitro studies by Scott et al[19] confirm the mutation R302Q to be associated with loss of enzymatic activity and suggest the mechanism to be decreased binding to AMP. The γ-2 subunit has 4 copies of a motif of 60 amino acids referred to as the CBS motif and occurs in tandem pairs to form the Bateman domain.[20] The Bateman domain is highly conserved across species, and in more than 1000 proteins, it is responsible for binding adenosyl compounds. Mutations in the CBS sequence are known to cause hereditary diseases, including homocystinuria, retinitis pigmentosa, congenital myotonia, epilepsy, hypercalciuric nephrolithiasis, and Bartter's syndrome.[20] All of these mutations are associated with loss of function of AMPK due to decreased affinity of the Bateman domain for AMP. In assays for cardiac AMPK activity, increasing concentrations of AMP were not accompanied by a corresponding increase in enzymatic activity, perhaps in keeping with previous studies that showed that mutations within the CBS domains of γ-2 interfere with AMP binding and activation of AMPK.[18,19] It is also significant that 3 other AMPK mutations known to cause WPW have also been shown in vitro to be associated with loss of enzymatic activity.[19] Thus, the mutation R302Q

occurring in a CBS motif prevents binding of AMP to the γ-2 subunit and is responsible for the phenotype of the transgenic animal model and the human phenotype in the families we have studied.[5] Arad et al[10] identified a mutation, N488I, in the *PRKAG2* gene to be responsible for WPW. This mutation is associated with increased AMPK activity. The phenotype of increased glycogen deposition is surprising because AMPK is well documented to inhibit glycogen synthesis. The authors suggest the mechanism is increased absorption of glucose. The human phenotype due to the mutation R302Q includes cardiac hypertrophy,[5] and reported families with other AMPK mutations have a similar if not higher incidence of ventricular hypertrophy.[6,7] The mechanism for the hypertrophy is most likely compensatory owing to insufficient ATP made available by the defective AMPK protein, as suggested by Doevendans and Wellens[21] and others.[22,23] However, the wild type also exhibited hypertrophy, which makes it less likely to be compensatory, but perhaps there is some energy deficiency even in the wild type due to decreased enzymatic activity of the human protein relative to that of the mouse.

In the mutant mice, but not in the wild-type or nontransgenic mice, we observed muscle bundles that extended from the atrium to the ventricle in the region of the fibrous body. It remains to be determined whether they are the accessory pathways responsible for electrical conduction bypassing the AV node. These are similar to the muscle bundles observed and reported by Arad et al.[10] Detailed pathological studies that involve sectioning of the AV ring and other portions of the conduction system will be required and are ongoing. Any suspected anatomic substrate will require testing for electrical conduction to prove or disprove its candidacy as the accessory pathway.

The mechanism whereby loss of AMPK activity induces the accessory pathway that leads to WPW remains uncertain. There is no doubt that the accessory pathway provides the requisite portion of the loop to give rise to reentrant supraventricular tachyarrhythmias. The supraventricular arrhythmia could be induced and clearly inhibited by blocking the accessory pathway. It is also evident that the mutation is necessary for the WPW phenotype, because it occurs only in mutant mice. The supraventricular tachycardia could reflect nodal reentry (AV nodal reentrant tachycardia); however, the evidence strongly suggests the accessory pathway is the mechanism. We have clearly demonstrated there is a functioning accessory pathway. The phenotype is identical to that observed in the families we have studied. In addition, the reentry tachycardia was consistently induced only after antegrade block of the accessory pathway during atrial extra-stimulus testing. If AV nodal reentrant tachycardia were inducible, one would expect to see some instances of tachycardia induced before accessory pathway block, and possibly bystander accessory pathway conduction during the tachycardia. These features were never observed, which provides strong evidence that AVRT was the mechanism of the tachycardia. Furthermore, the VA interval during tachycardia (18±4 ms) was similar to that during ventricular pacing, which was fixed and nondecremental (19±5 ms) in mutant mice, in line with retrograde conduction over the accessory pathway. In contrast, in wild-type mice, the VA interval was not fixed, and prolongation (decremental conduction) was observed at longer ventricular pacing cycle lengths.

In humans, there are several accessory pathways available for conduction at birth, but they disappear after a few weeks.[4] It is reasonable to assume the altered metabolic state in some way predisposes to the retention or development of the accessory pathway and subsequent WPW. One postulate is that the accessory pathways normally undergo apoptosis, but lack of AMPK activity prohibits it. There is also the possibility that the AMPK mutation induces de novo development of an accessory pathway. In the human phenotype, there is also progressive slowing of AV conduction, which not infrequently requires a pacemaker.[5] The gradual progression of conduction impairment in humans may be reflected in the present

mouse model by the slower resting heart rate and occasional atrial arrhythmias observed in the TG_{R302Q} mouse. The mechanism whereby conduction is impaired remains to be elucidated. The cardiac conduction system is more resistant to ischemia and other injury than myocytes, in part because of increased capacity for generation of ATP from glycolysis.[24] The loss of AMPK activity results in increased glycogen synthesis and less glucose available for generation of ATP. Light et al[25] have documented that the AMPK R302Q mutation resulted in slowing of open-state inactivation of the sodium channel and prolongation of action potential duration. This may be the explanation for impaired cardiac conduction. We have thus shown the primary defect is loss of AMPK activity due to a mutation that disturbs the AMP binding site. Studies are now under way, in conjunction with Light et al, to further ascertain why the accessory pathway develops and why other features, such as conduction abnormalities, are associated with loss of AMPK activity. Elucidation of the molecular network whereby loss of AMPK activity mediates WPW and other consequences has the potential to unravel therapeutic targets not just for the treatment of arrhythmias but also for conduction disorders, including hypertrophy.

Acknowledgments

This work was supported in part by an NIH training grant, HL-07706-10 (Dr Roberts), SCOR, 5P50-HL54313-09 (Dr Roberts), Modifier Grant, 5R01-HL068884-03 (Dr Marian), and Research Grant 5R01-HL068768-03 (Dr Khoury). We appreciate the administrative assistance of Deborah Graustein and Fran Baas in the preparation of this manuscript and figures. We also thank Dr Jeffrey Robbins for providing the α-myosin heavy chain promoter.

References

1. Dunnigan, A. Developmental aspects and natural history of preexcitation syndromes. In: Benditt, DG.; Benson, DW., editors. Cardiac Preexcitation Syndromes: Origins, Evaluation and Treatment. Boston, Mass: Martinus Nighoff; 1986. p. 21-29.
2. Wan W, Wu N, Fan W, Tang YY, Jin L, Fang Q. Clinical manifestations and prevalence of different types of supraventricular tachycardia among Chinese. Chin Med J 1992;105:284–288. [PubMed: 1618009]
3. Bauernfeind RA, Wyndham CR, Swiryn SP, Palileo EV, Strasberg B, Lam W, Westveer D, Rosen KM. Paroxysmal atrial fibrillation in the Wolff-Parkinson-White syndrome. Am J Cardiol 1981;47:562–569. [PubMed: 7468492]
4. James TN. Normal and abnormal consequences of apoptosis in the human heart: from postnatal morphogenesis to paroxysmal arrhythmias. Circulation 1994;90:556–573. [PubMed: 8026044]
5. Gollob MH, Green MS, Tang A, Ahmad F, Hassan A, Gollob T, Lozado R, Shah G, Tapscott T, Karibe A, Begley D, Mohiddin S, Fananapazir L, Bachinski L, Roberts R. Identification of a gene responsible for familial Wolff-Parkinson-White syndrome. N Engl J Med 2001;344:1823–1864. [PubMed: 11407343]
6. Arad M, Benson DW, Perez-Atayde A, McKenna WJ, Sparks EA, Kanter RJ, McGarry K, Seidman JG, Seidman CE. Constitutively active AMP kinase mutations cause glycogen storage disease mimicking. J Clin Invest 2002;109:357–362. [PubMed: 11827995]
7. Blair E, Redwood CS, Ashrafian H, Oliveira M, Broxholme J, Kerr B, Salmon A, Ostman-Smith I, Watkins H. Mutations in the gamma(2) subunit of AMP-activated protein kinase cause hypertrophic cardiomyopathy: evidence for the central role of energy comp disease pathogenesis. Hum Mol Genet 2001;10:1215–1220. [PubMed: 11371514]
8. Gollob MH, Seger JJ, Gollob TN, Tapscott T, Gonzales O, Bachinski L, Roberts R. Novel PRKAG2 mutation in the genetic syndrome of ventricular preexcitation and conduction defects with childhood onset and absence of cardiac hypertrophy. Circulation 2001;104:3030–3033. [PubMed: 11748095]
9. Cheung PC, Salt IP, Davies DG, Hardie DG, Carling D. Characterization of AMP-activated protein kinase gamma-subunit isoforms and their role in AMP binding. Biochem J 2000;346:659–669. [PubMed: 10698692]

10. Arad M, Moskowitz IP, Patel VV, Ahmad F, Perez-Atayde A, Sawyer DB, Walter M, Li GH, Burgon PG, Maguire CT, Stapleton D, Schmitt JP, Guo XX, Pizard A, Kupershmidt S, Roden DM, Berul CI, Seidman CE, Seidman JG. Transgenic mice overexpressing mutant PRKAG2 define the cause of Wolff-Parkinson-White syndrome in glycogen storage cardiomyopathy. Circulation 2003;107:2850–2856. [PubMed: 12782567]
11. Halse R, Fryer LG, McCormack JG, Carling D, Yeaman SJ. Regulation of glycogen synthase by glucose and glycogen: a possible role for AMP-activated protein kinase. Diabetes 2003;52:9–15. [PubMed: 12502487]
12. Patel R, Nagueh SF, Tsybouleva N, Abdellatif M, Lutucuta S, Kopelen H, Quinones M, Zoghbi WA, Entman ML, Roberts R, Marian AJ. Simvastatin induces regression of cardiac hypertrophy and fibrosis and improves cardiac function in a transgenic rabbit model of human hypertrophic cardiomyopathy. Circulation 2001;104:317–324. [PubMed: 11457751]
13. Berul CI, Aronovitz MJ, Wang PJ, Mendelsohn ME. In vivo cardiac electrophysiology studies in the mouse. Circulation 1996;94:2641–2648. [PubMed: 8921812]
14. Leitch JW, Klein GJ, Yee R, Feldman RD, Brown J. Differential effect of intravenous procainamide on anterograde and retrograde accessory pathway refractoriness. J Am Coll Cardiol 1992;19:118–124. [PubMed: 1729322]
15. Goy JJ, Fromer M. Antiarrhythmic treatment of atrioventricular tachycardias. J Cardiovasc Pharmacol 1991;17(suppl 6):S36–S40. [PubMed: 1723116]
16. Sharpe MD, Cuillerier DJ, Lee JK, Basta M, Krahn AD, Klein GJ, Yee R. Sevoflurane has no effect on sinoatrial node function or on normal atrioventricular and accessory pathway conduction in Wolff-Parkinson-White syndrome during alfentanil/midazolam anesthesia. Anesthesiology 1999;90:60–65. [PubMed: 9915313]
17. Sharpe MD, Dobkowski WB, Murkin JM, Klein G, Yee R. Propofol has no direct effect on sinoatrial node function or on normal atrioventricular and accessory pathway conduction in Wolff-Parkinson-White syndrome during alfentanil/midazolam anesthesia. Anesthesiology 1995;82:888–895. [PubMed: 7717560]
18. Daniel TD, Carling D. Functional analysis of mutations in the gamma 2 subunit of AMP-activated protein kinase associated with cardiac hypertrophy and Wolff-Parkinson-White syndrome. J Biol Chem 2002;277:51017–51024. [PubMed: 12397075]
19. Scott JW, Hawley SA, Green KA, Anis M, Stewart G, Scullion GA, Norman DG, Hardie DG. CBS domains form energy-sensing modules whose binding of adenosine ligands is disrupted by disease mutations. J Clin Invest 2004;113:274–284. [PubMed: 14722619]
20. Kemp BE. Editorial Bateman domains and adenosine derivatives form a binding contract. J Clin Invest 2004;113:182–184. [PubMed: 14722609]
21. Doevendans PA, Wellens HJ. Wolff-Parkinson-White syndrome. Circulation 2001;104:3030–3033. [PubMed: 11748095]
22. Roberts R, Marian AJ. Can an energy-deficient heart grow bigger and stronger? J Am Coll Cardiol 2004;41:1782–1785.
23. Crilley JG, Boehm EA, Blair E, Rajagopalan B, Blamire AM, Styles P, McKenna WJ, Ostman-Smith I, Clarke K, Watkins H. Hypertrophic cardiomyopathy due to sarcomeric gene mutations is characterization by impaired energy metabolism irrespective of the degree of hypertrophy. J Am Coll Cardiol 2003;41:1776–1782. [PubMed: 12767664]
24. Kubler W, Schomig A, Senges J. The conduction and cardiac sympathetic systems: metabolic aspects. J Am Coll Cardiol 1985;5(suppl):157B–161B.
25. Light PE, Wallace CHR, Dyck JRB. Constitutively-active AMP-activated protein kinase regulates voltage-gated sodium channels in ventricular myocytes. Circulation 2003;107:1962–1965. [PubMed: 12682004]

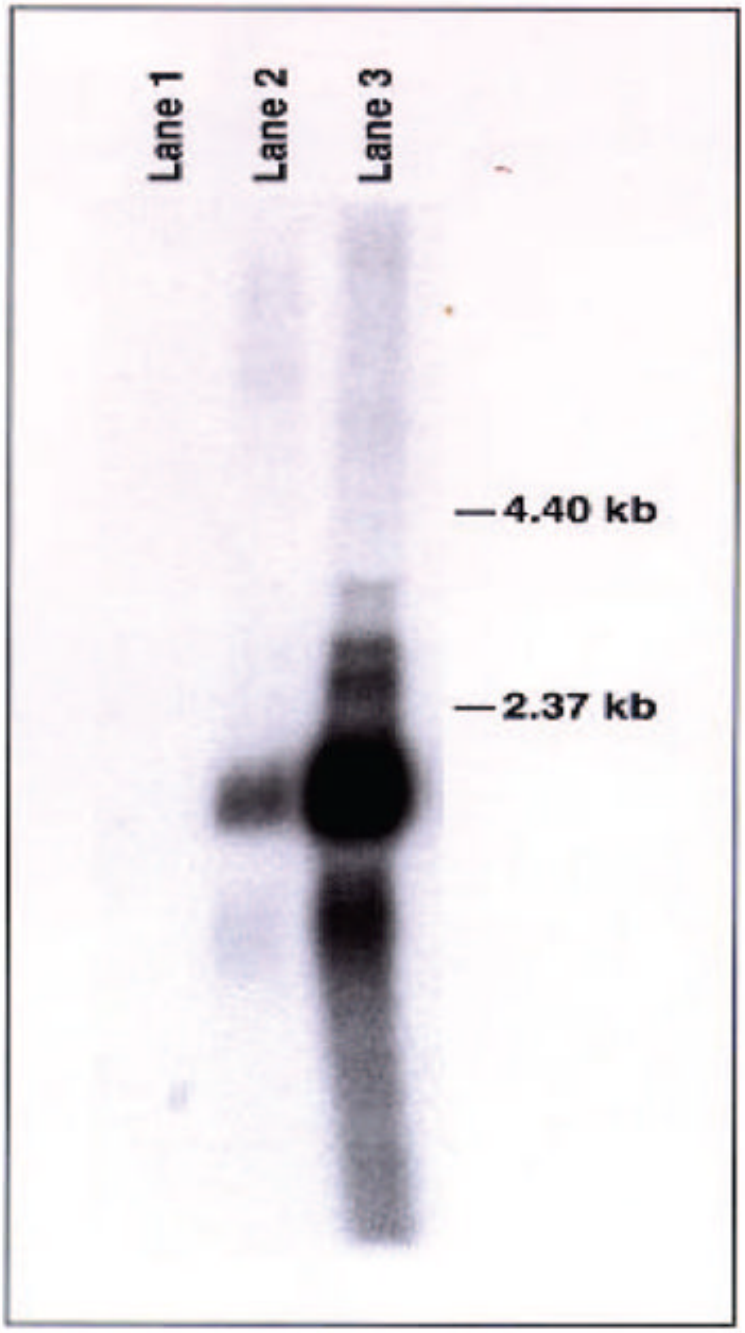

Figure 1.
Northern blot analysis of *PKRAG2* for cardiac expression. Expression was evident in transgenic, wild-type (lane 2), and mutant (lane 3) mice with absence of expression in non-transgenic mouse heart (lane 1).

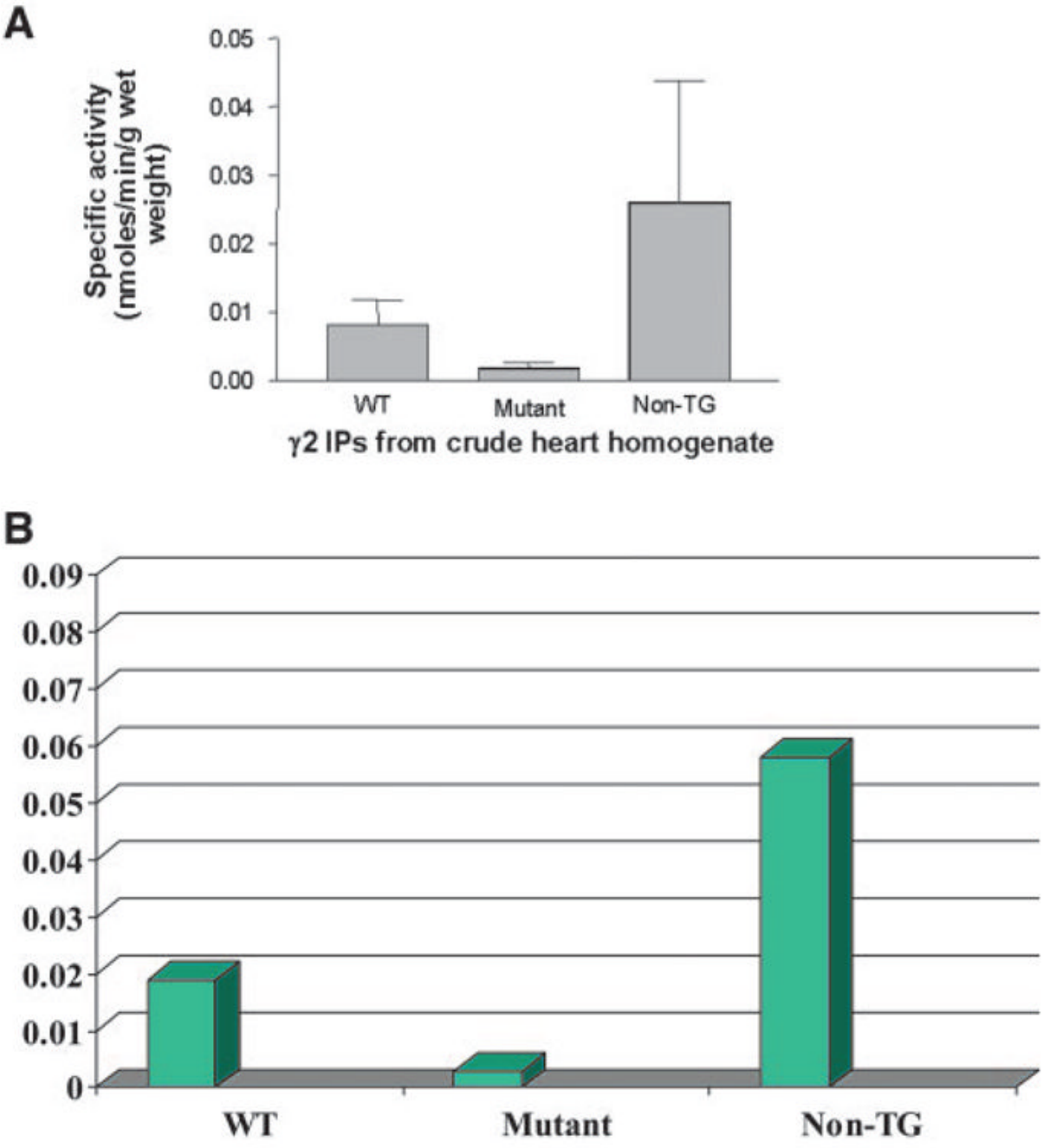

Figure 2.

A, Enzymatic activity of AMPK in myocardial tissue is shown for transgenic wild type (WT), mutant, and nontransgenic mice (non-TG). B, Total myocardial enzymatic activity of AMPK as detected by pan antibody to β-2 subunit is shown for transgenic wild-type (WT), mutant, and nontransgenic (non-TG) mice. Activity as detected by γ-2 antibody is expressed as mean±SD. Specific activity expressed as nmol $\cdot$ min^{-1} $\cdot$ g^{-1} wet weight is shown on ordinate, and 3 groups indicated on abscissa are wild-type (WT), mutant, and nontransgenic (non-TG) mice. IP indicates immunoprecipitate.

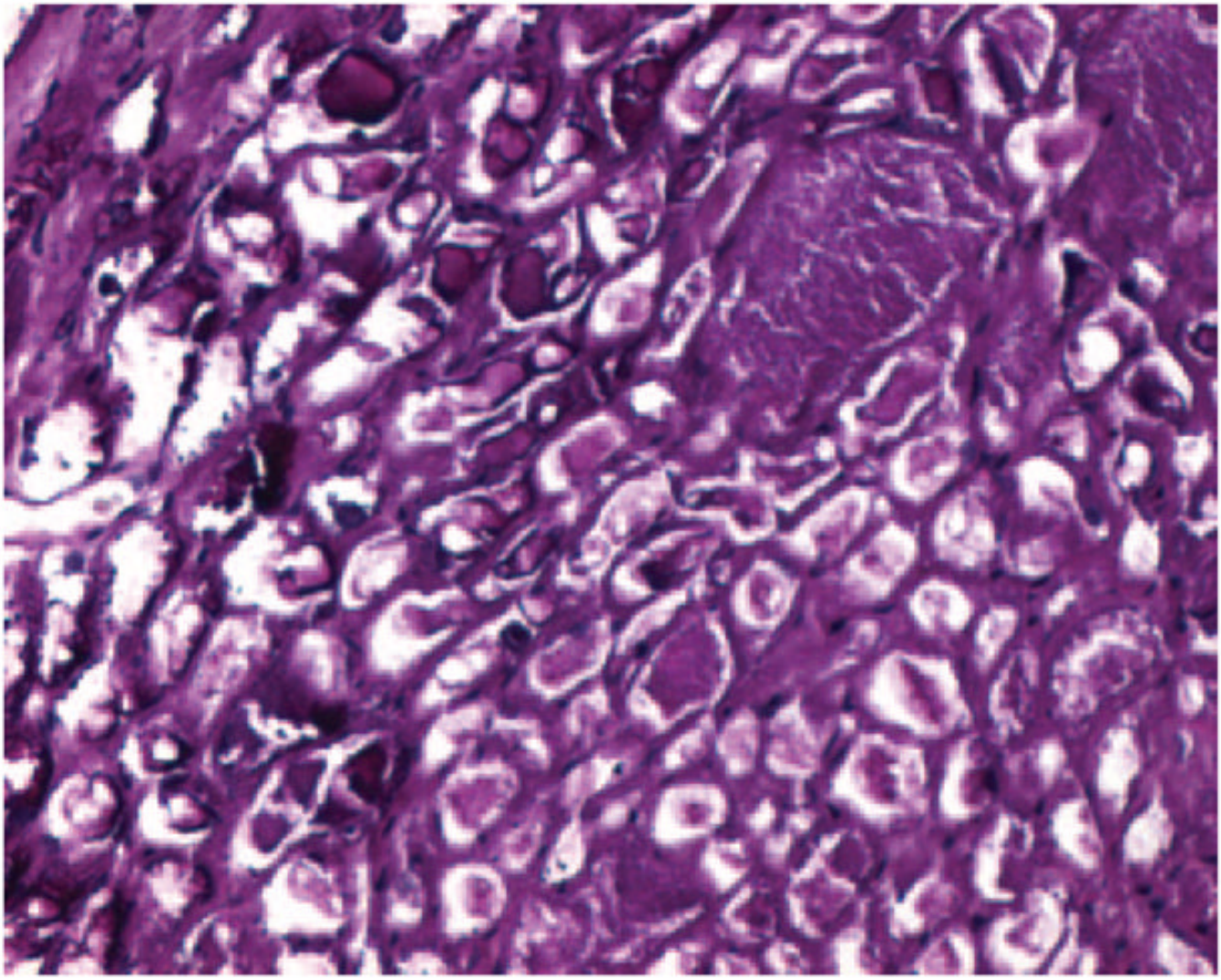

Figure 3.
Mutant, transgenic heart stained with PAS shows thickened wall with abundance of vacuoles. Vacuoles primarily contain PAS-positive material, which indicates increased deposition of glycogen.

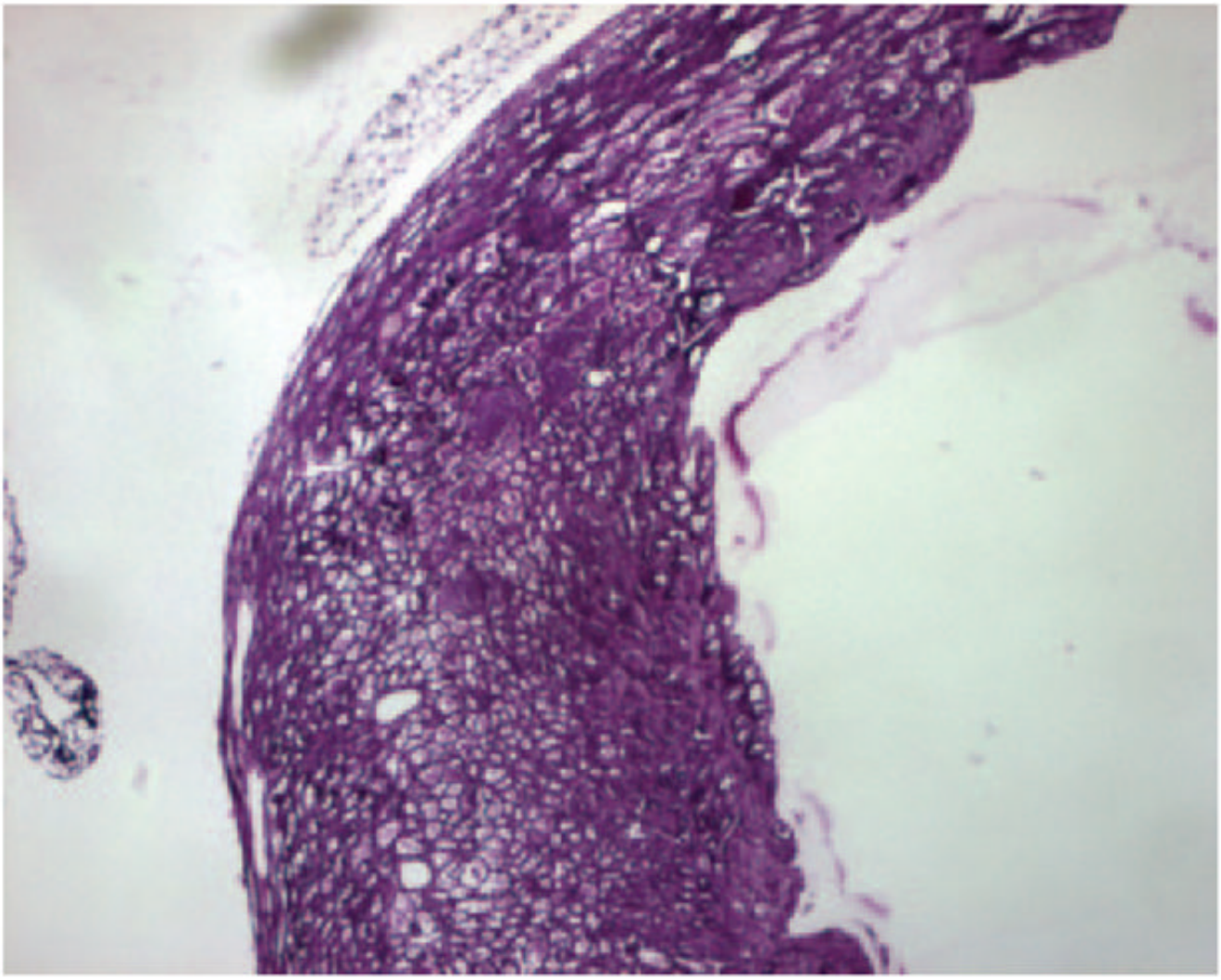

Figure 4.
Higher magnification of heart shown in Figure 3.

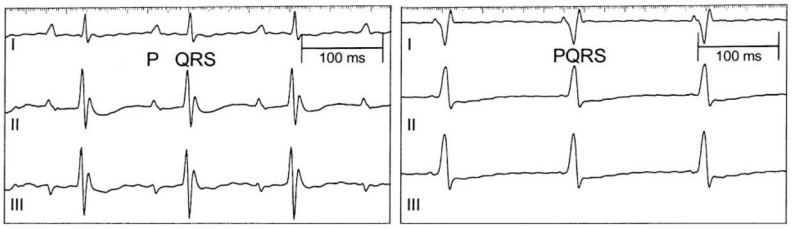

Figure 5.
Left, ECG of TG_{WT} mouse with normal PR and QRS intervals. Right, Tracings of TG_{R302Q} mouse with ventricular preexcitation evidenced by short PR interval and wide QRS duration.

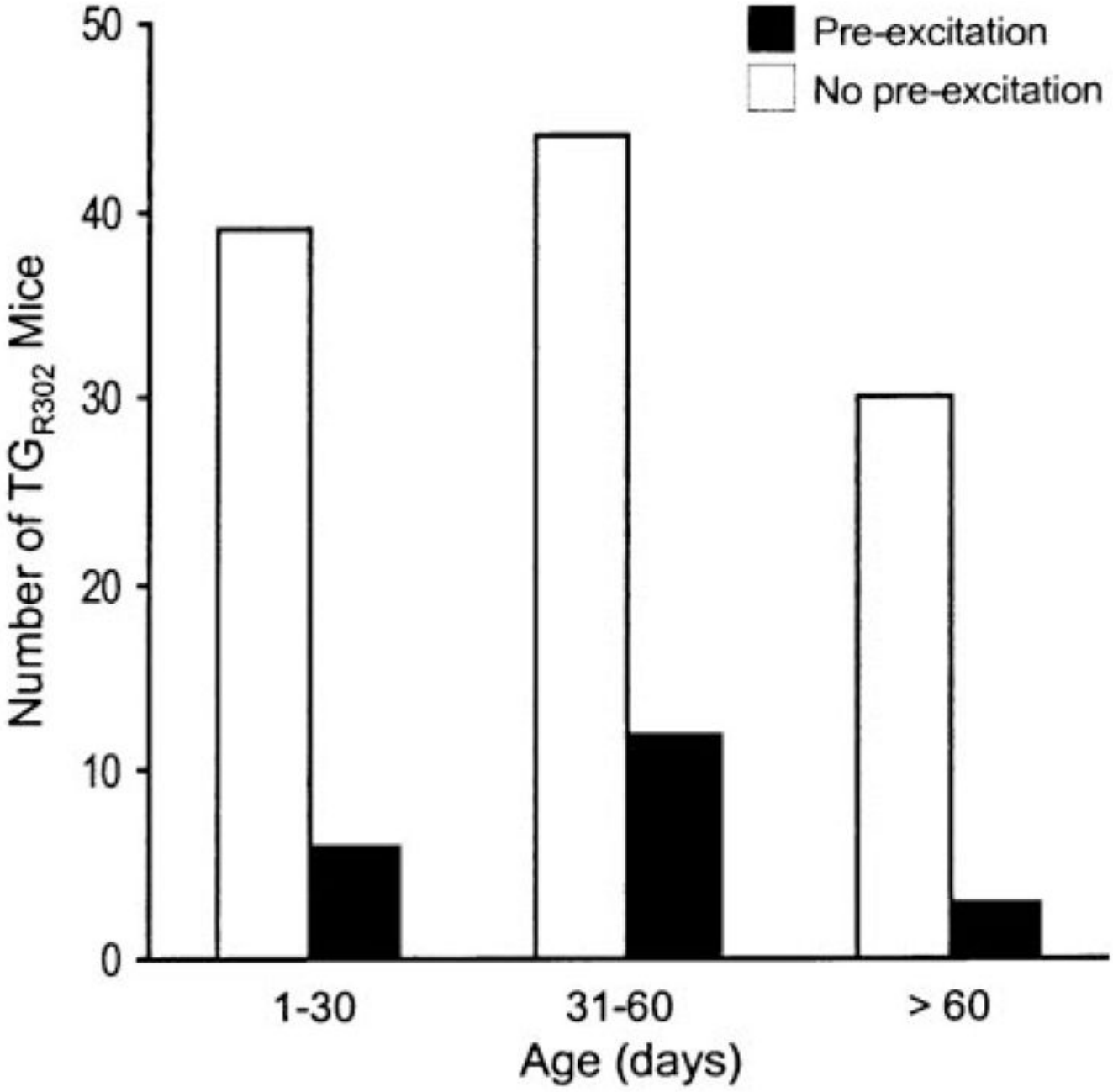

Figure 6.
Age distribution of TG_{R302Q} mice. Solid bars indicate number of mice exhibiting preexcitation on 3-lead surface ECG.

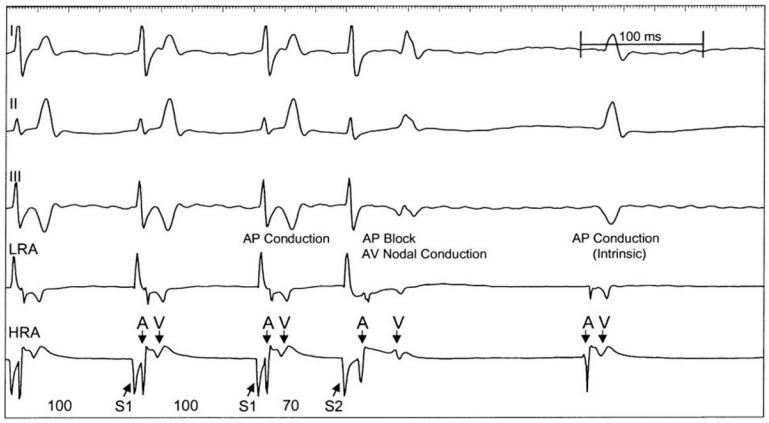

Figure 7.

Simultaneous ECG and intracardiac electrograms during atrial stimulation in TG_{R302Q} mouse with ventricular preexcitation. AV conduction propagated through accessory pathway during stimulation drive train (S1) delivered at cycle length of 100 ms. PR interval and QRS duration and morphology during S1 were similar to intrinsic rhythm. Premature extrastimulus (S2) delivered during accessory pathway refractoriness (70 ms after S1) caused AV conduction to proceed only through AV node, as evidenced by prolonged PR interval and narrowed QRS. LRA indicates low right atrial electrogram; HRA, high right atrial electrogram.

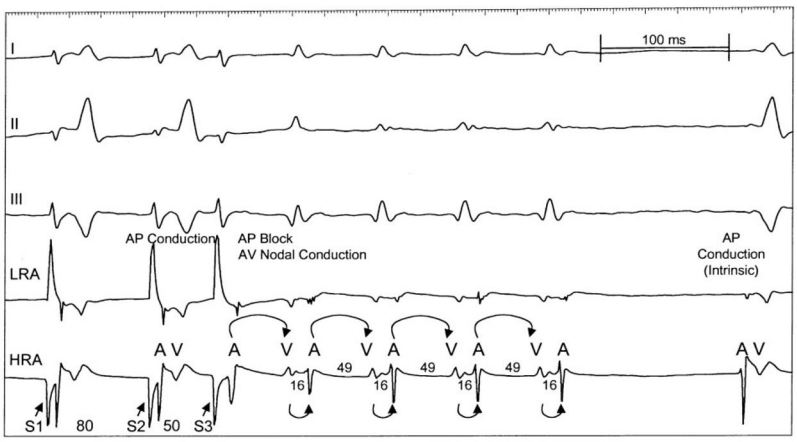

Figure 8.

Simultaneous ECG and intracardiac electrograms during orthodromic AV reentrant tachycardia induced by atrial stimulation in TG_{R302Q} mouse with ventricular preexcitation. After stimulation drive train (S1) at cycle length of 100 ms, 2 progressively premature extrastimuli were delivered at S1-S2 of 80 ms and S2-S3 of 50 ms. Conduction due to S3 was blocked at accessory pathway, with antegrade conduction only through AV node (long AV interval). After accessory pathway recovery from refractoriness, VA conduction was retrograde through accessory pathway (short VA interval), which completed the reentry loop. Reentrant tachycardia continued for a few beats until it self-terminated. LRA indicates low right atrial electrogram; HRA, high right atrial electrogram.

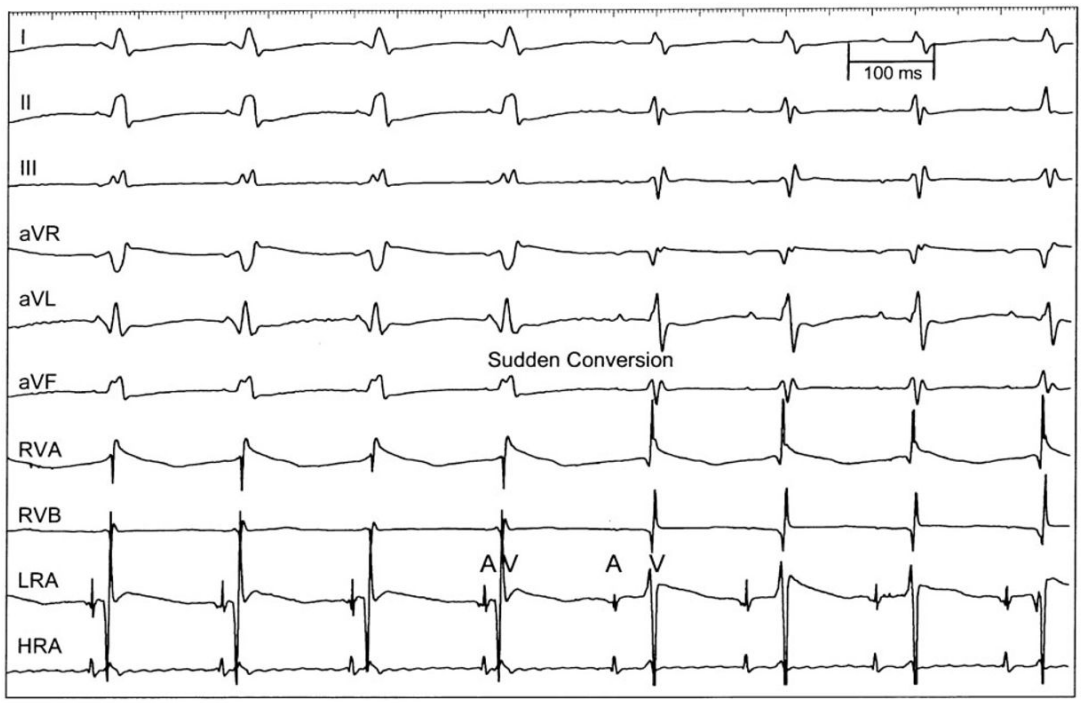

Figure 9.

Simultaneous ECG and intracardiac electrograms during procainamide administration in TG_{R302Q} mouse with ventricular pre-excitation. Procainamide resulted in sudden block of accessory pathway 3 to 5 minutes after intravenous infusion, as evidenced by spontaneous PR interval prolongation and QRS narrowing. RVA indicates right ventricular apical electrogram; RVB, right ventricular basal electrogram; LRA, low right atrial electrogram; and HRA, high right atrial electrogram.

Table

Echocardiographic Comparison of Nontransgenic, Wild-Type Transgenic (TG_{WT}), and Mutant Transgenic (TG_{R302Q}) Mice

Echocardiographic Parameter	Nontransgenic Mice (n=11)	Wild-Type Mice (n=15)	Mutant Mice (n=12)	*P*, 1-Way ANOVA	*P*, Kruskal Wallis (Mutant/ Nontransgenic)	*P*, Kruskal Wallis (Mutant/Wild-Type)
Average PWT, cm	0.09	0.13	0.12	0.001	0.007	0.195
Average EDD, cm	0.33	0.38	0.43	0.004	0.011	0.261
Average ESD, cm	0.20	0.26	0.31	0.002	0.003	0.107
Average FS, %	42	32	29	0.010	0.011	0.354

PWT indicates posterior wall thickness; EDD, end-diastolic diameter; ESD, end-systolic diameter; and FS, fractional shortening.